13th ewtec 2019 Proceedings of the 13th European Wave and Tidal Energy Conference 1-6 Sept 2019, Naples, Italy

# Wave-turbulence separation with empirical orthogonal function analysis

Michael Togneri, Ian Masters, and Iain Fairley

*Abstract*—**Tidal turbine reliability is strongly affected by fluctuating loads induced by turbulence and waves at tidal energy sites. Turbulence is most often characterised through its intensity, which is the turbulent kinetic energy (TKE) scaled by the mean flow speed. The most common instrument for measuring TKE is the acoustic Doppler current profiler; however, the estimate from this instrument is intrinsically contaminated by wave action, and in fact wave action may completely swamp the true turbulence. We describe a statistical signal separation method based on empirical orthogonal function analysis, and apply it to a test case that performs well in separating the true TKE from the pseudo-TKE induced by the waves. The validity of the method is tested against estimates from linear theory, using wave state parameters from a wave buoy operating independently of the profiler. We find that estimates are very well-correlated with one another, but error between theoretical and statistical estimates of wave action can appear very high unless low wave height conditions are excluded. A decomposition of the original TKE estimate into wave and turbulence components, based only on the profiler data, is presented.**

*Keywords*—**empirical orthogonal functions, tidal energy, turbulence, waves, currents.**

## I. Introduction

THE combined action of waves and turbulence in energetic tidal currents is the strongest contributor to load variability on tidal energy converters (TECs) [1-3]. Quantifying these phenomena from field measurements at actual or potential deployment sites, however, is not a trivial task. The most widely-employed tools for measurement of flow conditions, and those recommended in IEC standards [4], are acoustic Doppler current profilers (ADCPs). There are many different techniques available to estimate turbulence and wave properties using data from ADCPs or similar acoustic devices [5-7]; in the current paper, we focus on measurement of turbulence kinetic energy (TKE), which is most often estimated using the variance method [8,9].

An important shortcoming of the variance method is that, since it is based on measurements of velocity variance, any source of variance other than the turbulence will include information about both turbulence and any other contributing phenomena. Most significantly, this means that the variance associated with orbital wave motions is also included. Thus, estimates of TKE obtained from ADCPs are biased high by wave action, sometimes so much so that the true TKE is an order of magnitude smaller than the estimated value [10].

We therefore have a situation where we wish to analyse a dataset that simultaneously measures two different physical phenomena in a single parameter, with no *a priori* means of disentangling them on purely physical grounds. However, the strong dominance of the wave contribution at times of significant wave activity suggests that empirical orthogonal function (EOF) analysis could provide a solution. EOF analysis picks out the statistically dominant basis functions from a spatiotemporal data set; if wave activity is indeed as strong as it appears to be from inspection, then the most important basis function should capture almost all its contribution.

In this paper, we present a method to separate out waves and turbulence from ADCP estimates of turbulent kinetic energy, and show the results of applying this method to a real data set. Section II gives details of the data collection, and presents a short introduction to the methods of data analysis. The ability of the EOF analysis to pick out wave effects from the coupled data is tested by comparison to linear wave theory; a brief discussion of the relevant theory is also shown in section II. In section III we present the key findings from the example data set. Finally in section IV we assess the usefulness of the method, and highlight its key strengths and weaknesses.

## II. Method

### A. Data set and instrumentation

The data for this paper is taken from a campaign carried out in the Morlais Demonstration Zone (MDZ) off the coast of Anglesey in Wales. We use measurements from an RDI

Paper ID number: 1243
Paper track: TRC (Wave/tidal resource characterisation)
M. Togneri acknowledges the support of the Welsh Assembly Government through the Sêr Cymru National Research network for Low Carbon, Energy and Environment, of EPSRC through the project SURFTEC (EP/P008628/1) and of ERDF through the Interreg Atlantic Area project MONITOR (EAPA_333/2016). The data were collected as part of, and I. Fairley acknowledges the financial support of the SEACAMS and SEACAMS 2 projects, part-funded by the European Regional Development Fund through the Welsh Government.
M. Togneri (M.Togneri@swansea.ac.uk), I. Masters (I.Masters@swansea.ac.uk) and Iain Fairley (I.A.Fairley@swansea.ac.uk) work in the Energy and Environment Research Group of the College of Engineering in Swansea University.

  

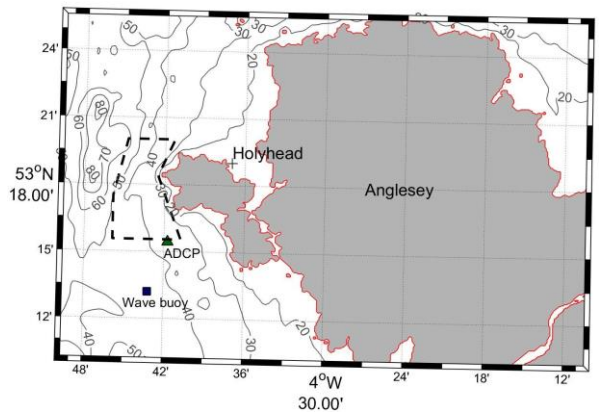


Fig. 1. Location of the ADCP and buoy relative to the MDZ, whose boundary is shown as a dashed line. Bathymetry contours show depth relative to mean sea level. Image credit: S. Neill

Sentinel V ADCP deployed on the southern edge of the MDZ between 19/09/14 and 19/11/14. In addition to the ADCP, we also use data from a wave buoy on a longer deployment that fully overlaps the ADCP deployment period. This buoy was located approximately 2km to the south of the MDZ (see fig. 1). Peak spring depth range was approximately 5m (41.1 - 46.2m), and the depth-averaged peak spring current was 2.5ms$^{-1}$.

The ADCP measured a 15 minute burst of data every hour at a sample rate of 2Hz; the ping frequency was 614.4kHz. Throughout the rest of this paper, all data from a given burst will be represented by a time-average value for the whole burst. The vertical bin size was 0.6m and the blanking distance at the bed was 1.89m; the beam angle was 25° from vertical. Wave buoy measurements corresponding to ADCP measurements from any particular burst are represented by an average across the same 15-minute period. More details of the site and data collection can be found in [10-12].

### B. *Estimation of TKE from ADCP data*

We have referred to the parameter that we are estimating as the turbulent kinetic energy (TKE), although more precisely it is the TKE per unit mass. This is denoted $k$, and is related to the Cartesian velocity components ($u$,$v$,$w$) by:

$$k = \frac{1}{2}(\langle u'^2\rangle + \langle v'^2\rangle + \langle w'^2\rangle), \tag{1}$$

where angle brackets denote a time average over a burst and a prime denotes the fluctuating component.

Although the Sentinel V has five beams (one vertical and four off-vertical), following the work presented in [13] we note that using the fifth beam does not significantly alter the estimate of TKE and introduces greater uncertainty. Thus, we use a four-beam estimate of TKE for the rest of this paper. A detailed description of the estimation method can be found in [8] or [14], but in short if we take the velocity along the $i$th beam to be $b_i$, then its variance is $\langle b_i'^2\rangle$. Using certain simplifying assumptions about the behaviour of turbulence across the area sampled by the beams, we can produce an ADCP estimate of $k$ from the beam variances as:

$$k_{ADCP} = \frac{\sum_{i=1}^{4}\langle b_i'^2\rangle}{4\sin^2\theta\,(1-\xi(1-\cot^2\theta))}, \tag{2}$$

where $\theta$ is the inclination angle of the off-vertical beams and $\xi$ parametrises the turbulent anisotropy.

As noted in section I, this method produces an estimate of $k$ which assumes that all variance in the beam velocities is due to turbulent fluctuations. If waves (or some other flow phenomenon) creates additional velocity variation, the estimated quantity $k_{ADCP}$ will not measure TKE, but rather a related quantity that captures both the true TKE and a "pseudo-TKE" due to wave action. Under the assumption that there is no significant statistical correlation between waves and turbulence, their contributions can be regarded as superposed on one another, which means we can simply regard $k_{ADCP}$ as a sum of the turbulent and wave contributions:

$$k_{ADCP} = k_t + k_w. \tag{3}$$

In this formulation, $k_t$ is the true TKE and $k_w$ the pseudo-TKE component of the ADCP estimate of $k$.

### C. *Velocity variance in linear wave theory*

In Airy wave theory, the horizontal ($u$) and vertical ($w$) components of orbital velocity for a given wave state can be expressed using a velocity potential such that $u = \partial\varphi/\partial x$ and $w = \partial\varphi/\partial z$, where

$$\varphi(x,z,t) = \frac{\sigma}{\kappa}\,a\,\frac{\cosh(\kappa(z+h))}{\sinh(\kappa h)}\sin(\kappa x - \omega t) \tag{4}$$

Here, $x$ and $z$ express spatial position (note that $z$ is depth from surface), $t$ is time, $a$ is wave amplitude, $\kappa$ is wavenumber, and $\omega$ and $\sigma$ are observed and intrinsic frequency respectively. On this basis, the expected wave pseudo-TKE will be:

$$k_w = \frac{1}{4}\frac{\sigma^2 a^2}{\sinh^2(\kappa h)}\sinh^2(\kappa(z+h)) \tag{5}$$

The wave properties $a$, $\kappa$, $\omega$ and $\sigma$ were obtained from the wave buoy. Of these, the buoy only directly measures observed frequency $\omega$ and significant wave height, which we divide in half to get $a$. To calculate $\kappa$ we take $\omega$ and the buoy's measurement of wave direction, along with the ADCP's measurements of water depth, surface current speed and direction, and use these in the dispersion relation. It is then relatively trivial to calculate $\sigma$. This gives us all the data we need to fully specify the expected pseudo-TKE profiles due to linear waves as given in (5).

### D. *EOF analysis*

EOFs are a well-established technique for analysing climatic and meteorological data, so we do not propose to

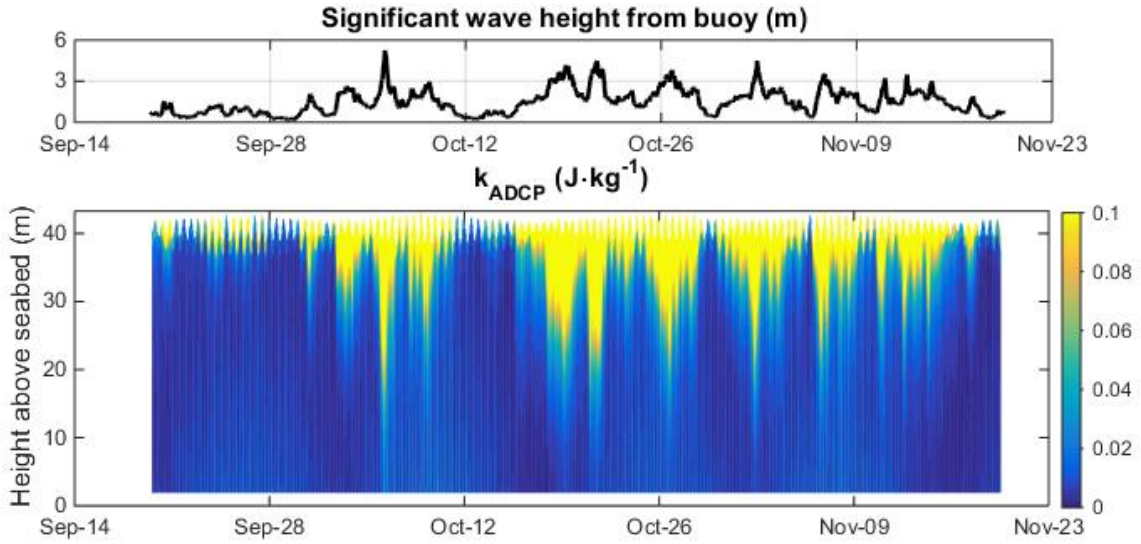


Fig. 2: Bottom panel shows pseudo-TKE as estimated from ADCP data using (2) for the whole deployment. Top panel shows the concurrent buoy measurements of significant wave height. The colour map has been truncated to improve visibility of low $k_{ADCP}$ values. Figure adapted from [10].

describe them in detail here. Reference [14] is a very helpful introductory manual for the interested reader; there are also more comprehensive texts that describe the method in greater detail [15,16].

In brief, EOF analysis decomposes a spatiotemporal dataset into a set of spatial basis functions (these basis functions are themselves the EOFs) which can be combined linearly to reconstruct the time-varying portion of the original data set. The weight of each basis function at a given time is given by the time-varying "expansion coefficient". If we have some spatiotemporal $D(\boldsymbol{x},t)$ that is decomposed into $N$ basis functions $\mathrm{EOF}_i(\boldsymbol{x})$ and expansion coefficients $\mathrm{EC}_i(t)$, with $i = 1,\dots,N$, then the original data can be fully reconstructed as:

$$D(\boldsymbol{x},t) = \sum_{i=1}^{N} \mathrm{EOF}_i(\boldsymbol{x}) \times \mathrm{EC}_i(t). \tag{6}$$

Here $N$ is the number of points in the spatial grid. Generally, we do not use the entire decomposition; instead it is possible to order the EOFs in terms of their relative contribution to the total variability of $D$, and work with a partial reconstruction of the dataset that, if performed appropriately, captures all significant dynamical behaviours. As the wave contribution to total ADCP estimate of TKE is seen to significantly dominate the turbulence contribution at times of strong wave activity, we expect that the first EOF will correspond almost entirely to the pseudo-TKE from wave action. If this is indeed the case, then the value of $\mathrm{EC}_1$ at any particular time will indicate whether wave-generated pseudo-TKE is a significant contribution to $k_{ADCP}$ at that time: a high positive value will indicate that waves are acting to positively bias $k_{ADCP}$, while a low or negative value will indicate that wave action is negligible.

As noted above, this decomposition captures only the time-varying component of the original data. Thus, it cannot be used to determine any bias in the mean value of $k_{ADCP}$ introduced by the waves. To fully capture the wave contribution, we must also estimate the mean bias that wave action introduces. Let us recast (3) in terms of the mean and time-varying contribution from waves and turbulence as:

$$\begin{aligned} k_{ADCP} &= \overline{k_{ADCP}} + \widetilde{k_{ADCP}} \\ &= (\overline{k_t} + \widetilde{k_t}) + (\overline{k_w} + \widetilde{k_w}). \end{aligned} \tag{7}$$

Here, an overbar indicates a mean value and a tilde indicates the time-varying component. These apply over the whole two-month dataset, cf. the $\langle\cdot\rangle$ and $\cdot'$ notation which were applied to data within a single 15-minute burst in (1) and (2).

If our EOF approach is correct, then $\mathrm{EOF}_1(\boldsymbol{x}) \times \mathrm{EC}_1(t) \approx \widetilde{k_w}$. However, we still need an estimate of $\overline{k_w}$ if we are to fully separate waves and turbulence. We achieve this by assuming that the first EOF does indeed capture the variability in total pseudo-TKE due to wave action – in this case, $\mathrm{EC}_1(t) < 0$ corresponds to times when wave action is not significant. A mean profile of $k_{ADCP}$ calculated from a subsample containing only these times will then be equal to $\overline{k_t}$, and we can then calculate $\overline{k_w} = \overline{k_{ADCP}} - \overline{k_t}$. This, in principle, allows us to separate out all four components on the right-hand side of (7).

The EOF method requires a dataset in which the spatial points are the same for each timestep; since the water depth changes throughout the cycle we must truncate the data prior to carrying out the EOF analysis. We elect to do this by truncating downwards from the highest point in the water column containing valid data, such that each successive burst contains the same depth range relative to the surface. This choice is made on the grounds that wave action extends downwards through the water column, so defining the data set such that its location relative to the point of maximum wave activity is fixed will make the

EOF analysis more likely to pick out modes that correspond to genuine wave phenomena.

## III. RESULTS

Fig. 2 shows the distribution of the ADCP estimate of TKE across all water depths for the whole deployment period, and compares it to the significant wave height during the same period. There is a clear coincidence of high waves and high values of $k_{ADCP}$ near the surface; this indicates that the most significant statistical mode is more likely to be strongly correlated with wave action.

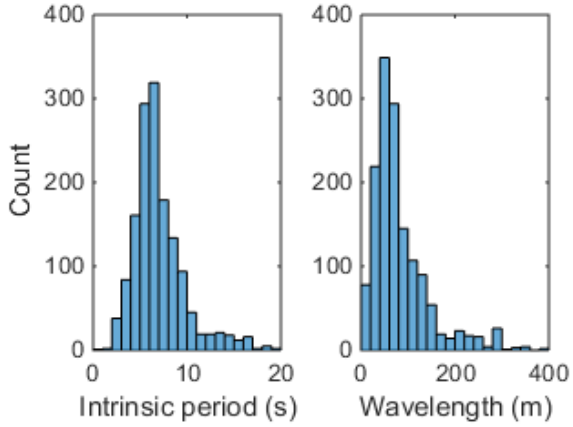


Fig. 3: Distributions of wave period and wavelength calculated from buoy measurements for the ADCP deployment period

The probability distributions of certain important wave properties are shown in fig. 3 – specifically, the intrinsic wave period and wavelength across the ADCP deployment. We see that the distributions show fairly sharp peaks – quantitatively, the kurtosis of the period distribution is 5.99 and that of the wavelength distribution is 7.43. Most wave observations have a period in the range 6.5±1.4s and a wavelength in the range 65±26m; this is consistent with swell for the location of the MDZ.

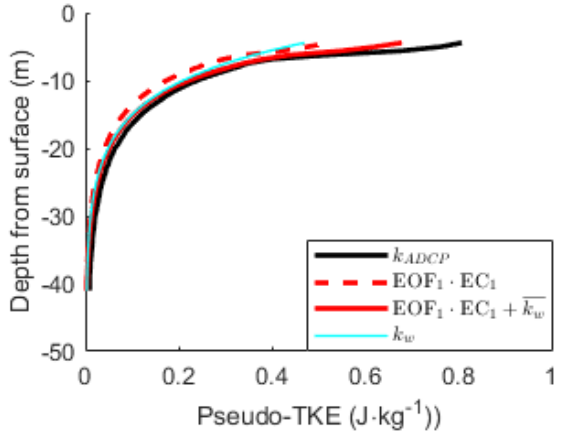


Fig. 4: Profiles of $k_{ADCP}$ and estimates of pseudo-TKE from an arbitrarily-chosen burst (18/10/14 1200-1215).

As an initial sanity check, before carrying out a more detailed analysis, it is worthwhile to examine whether the method proposed here produces results that appear plausible. In fig. 4, we show profiles of pseudo-TKE corresponding to a single arbitrarily chosen burst, alongside the total ADCP estimate of TKE. These profiles show the amount of the TKE estimate that is explained by $\mathrm{EOF}_1$ (with and without the addition of the estimated $\overline{k_w}$ value), and also the Airy wave theory estimate of wave pseudo-TKE according to the method described in section II-C. From this figure, we see that there is no obvious mismatch between the methods: the EOF estimate does not exceed the total $k_{ADCP}$ at any point (which would imply a negative value of $k_t$), and the linear-theory estimate of $k_w$ is clearly of the same order of magnitude as the EOF estimate.

The difference between the solid and dashed red lines in fig. 4 is the estimated value of $\overline{k_w}$, i.e., the mean bias introduced into the ADCP measurement of pseudo-TKE by wave action. Recall that we obtain this by the decomposition of the time-mean portion $\overline{k_{ADCP}}$ of the total measured pseudo-TKE, as proposed in section II-D and summarized by (7). The results of this decomposition are shown in more detail in fig. 5

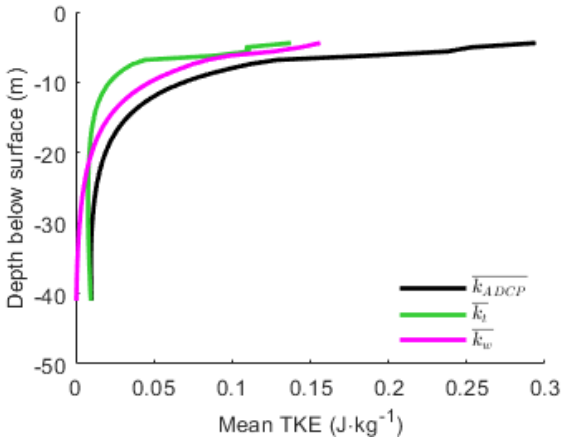


Fig. 5: Time-mean profile of the ADCP estimate of TKE, and its components due to wave and turbulent action, estimated using the method described in section II-D.

The decomposition is not completely satisfactory. We can see that the filtering the mean $k_{ADCP}$ profile by the proposed low-wave criterion (i.e., $\mathrm{EC}_1(t) < 0$) has yielded an estimated $\overline{k_t}$ profile that is mostly constant in the lower part of the water column, at depths below ca. 18m. However, closer to the surface, in a depth range roughly between 5-15m, the profile exhibits obviously wave-like behaviour. The estimated $\overline{k_w}$ profile is closer to what would be expected: it is a good approximation to a $\sinh^2$ function, as we would predict from (5). However, it is difficult to assess exactly how good this profile shape is; its goodness of fit will depend on the appropriate value of the wavelength $\kappa$. This parameter varies in time, and so there is no clear way to specify a single correct value for a profile that involves data from many different times.

Having looked at a single point in time, and briefly at the properties of the time average, we now proceed to examine how $k_{ADCP}$ varies throughout the measurement period. Fig. 6 compares the significant wave height with estimates of wave-generated pseudo-TKE $k_w$ from the

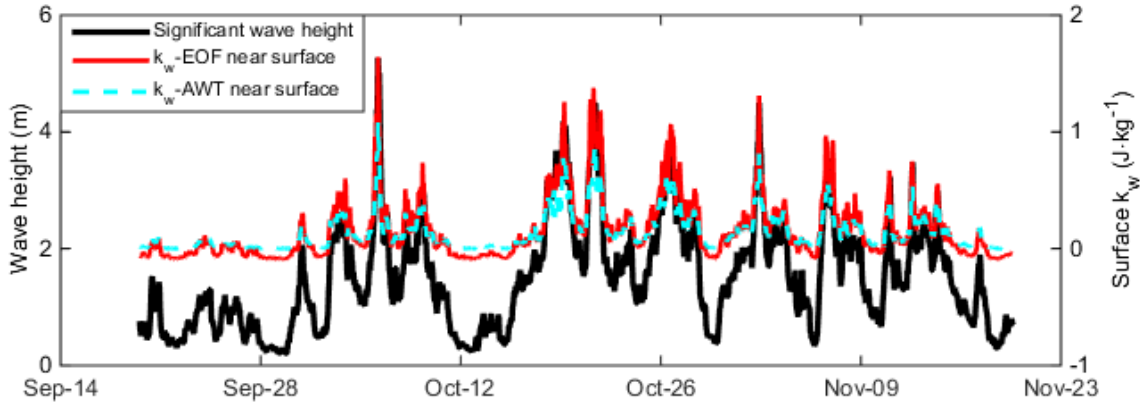


Fig. 6: Comparison of (left axis) significant wave height as measured from buoy with (right axis) near-surface wave pseudo-TKE estimated using EOF analysis ($k_w$-EOF) based on ADCP measurements, and Airy wave theory ($k_w$-AWT) based on wave buoy measurements.

EOF method and from Airy wave theory at a depth slightly below the surface. The depth chosen is the point closest to the surface that it is possible to obtain data from using an ADCP before sidelobe interference means that accurate measurement is no longer possible [17,18]; it is also the upper limit of the profiles shown in figs. 4 and 5. It is apparent that all three of these time series track one another quite closely, particularly when the significant wave height is above approximately 2m. This correlation is quantitively very good: the Pearson correlation coefficient for any pair of these three variables is in the range 0.94-0.96.

Rather than tracking a single value near the surface, we can get a more holistic assessment of the agreement between the two different estimates of wave pseudo-TKE by examining the depth-mean error between the estimates, as shown in fig. 7. The absolute error is not very large (compare the sample and mean profiles in figs. 4 and 5 for an idea of the typical pseudo-TKE values encountered in the data), but it is clear that the relative error can become very high, even when the absolute error is quite small. This is simply due to the fact that one estimate or the other can become very small without the other doing so. The result is that the relative error spikes extremely high, and the exact times at which it does so depends on whether we choose to calculate the relative error with the EOF estimate or the linear theory estimate on the denominator. A simple time average of the percentage error between the two estimation methods, then, will be very high due to these spikes. To better understand the importance of these very high relative errors, it is instructive to examine the relationships between errors and other flow parameters.

The size of the absolute error between the different estimates of $k_w$ is an important part of the context for understanding the behaviour of the relative error. In fig. 8, we show how the absolute error depends on key wave parameters, and on the near-surface value of the estimated pseudo-TKE itself. The relationships between error and wave period and wavelength are not immediately apparent, but in short, the peaks in error in panels (a) and

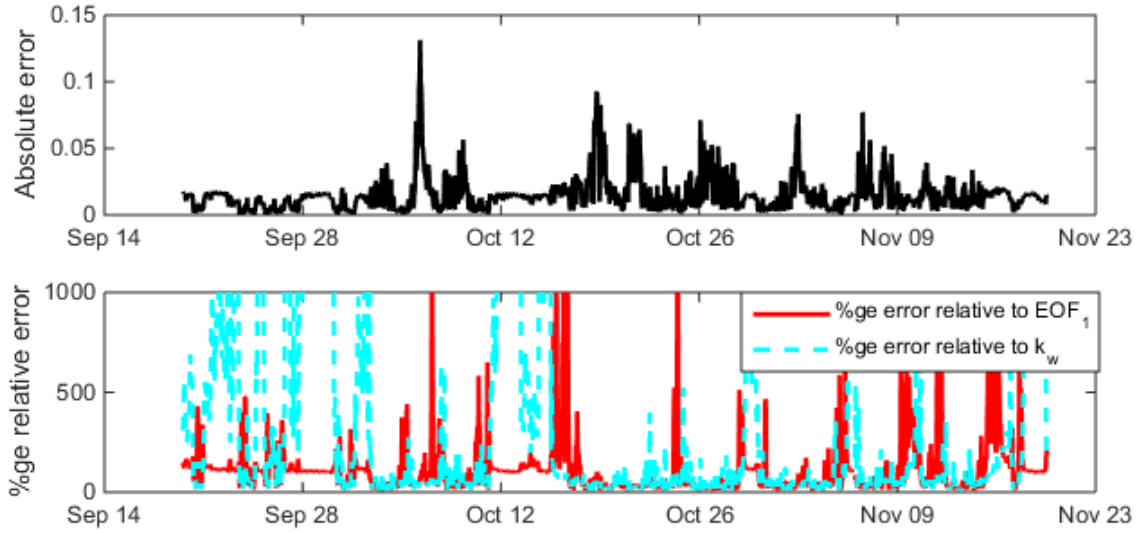


Fig. 7: Overview of error between the EOF and linear theory estimates of wave-generated pseudo-TKE, throughout the entire measurement period. Top panel shows the mean absolute error (in $Jkg^{-1}$) throughout the whole measured depth; bottom panel shows the relative error as a percentage.

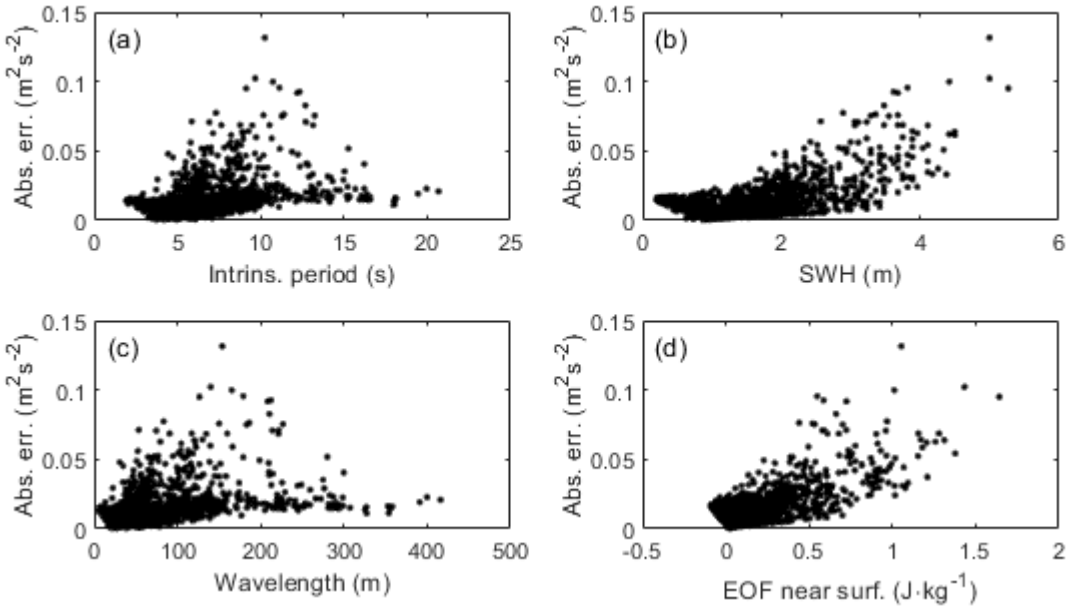


Fig. 8: Dependence of absolute error on (a) intrinsic wave period (b) significant wave height (c) wavelength (d) EOF estimate of near-surface wave pseudo-TKE (i.e., $k_w$-EOF, cf. fig. 6).

(c) approximately coincide with the most energetic wave conditions. The dependence of absolute error on wave height is more straightforward: panel (b) shows an approximately quadratic relationship between error and significant wave height (cf. the wave amplitude term in (5)). Most simple, however, is the change in error with respect to the magnitude of the estimated pseudo-TKE: there is an approximately linear relationship between error and near-surface pseudo-TKE estimates. For the EOF-based estimate shown in panel (d), the correlation is $R$ = 0.63; we do not show the relationship with the Airy wave theory estimate ($k_w$-AWT) as it is very similar, but the correlation in that case is even stronger ($R$ = 0.70).

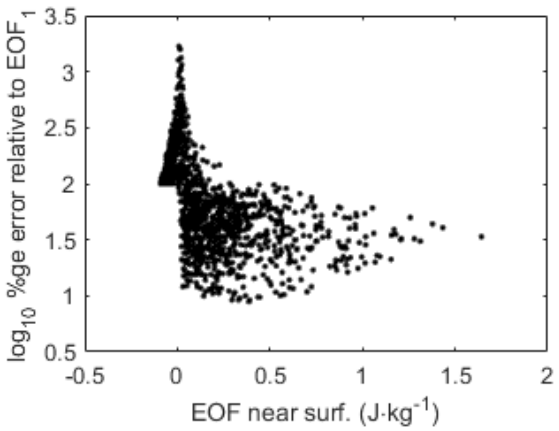


Fig. 9: Dependence of relative error on EOF estimate of near-surface wave pseudo-TKE.

These results should be borne in mind when interpreting the behaviour of the relative error as seen in fig. 9. This shows a very high peak in relative error, on the order of 1000%. However, it is clear that these very high errors occur only when the EOF estimate of wave pseudo-TKE is near zero. Comparing this to fig. 8(d), we see that the absolute error for these bursts is not behaving unusually, and that therefore the spike in relative error is purely due to very small values of the denominator in its calculation.

This means that attempts to calculate $k_w$ from theory or by EOF analysis are only robust when the wave pseudo-TKE is quite large. By a robust estimate of $k_w$ we mean one that can be well-corroborated between the two methods. This suggests, then, that using either of these methods to estimate the wave contribution to the total pseudo-TKE estimate obtained using (2) is only suitable at times when the wave contribution $k_w$ is sufficiently strong, and may provide erroneous or unhelpful estimates otherwise. If we assume that a very high error between the two estimation methods indicates a time at which both methods are returning an unsuitable estimate of $k_w$, then we can consider a criterion for selecting good $k_w$ estimates based on this error.

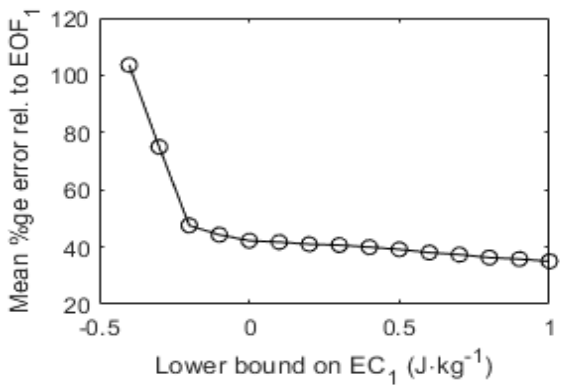


Fig. 10: Effect on mean relative error of filtering bursts by excluding those below a certain $EC_1$ limit.

This selection criterion should ideally be possible to choose *a priori*, without knowledge of the data set. Bearing this constraint in mind, the most intuitive choice is to say that suitable estimates of $k_w$ are only obtained when the expansion coefficient of the first EOF mode of the $k_{ADCP}$ date set is positive i.e., when $EC_1 > 0$. This criterion corresponds to the first EOF mode (whose magnitude we have seen closely tracks the wave height) being greater than zero. Fig. 10 shows that filtering the dataset by excluding bursts whose $EC_1$ value is below a certain threshold has a significant impact on the mean error, and that if we set this threshold to zero the mean error between the $k_w$-AWT and $k_w$-EOF is approximately 42%.

Finally, in fig. 11 we show the separated turbulent and wave contributions to the total ADCP estimate of TKE, $k_{ADCP}$. The two panels of this figure show the $k_{ADCP}$ dataset plotted in the bottom panel of fig. 2 decomposed according to (3) – this means that summing the two panels will perfectly recover the original dataset. At several points, one or other of the contributions takes a value below 0. This is not physically meaningful, but is instead an artefact of the decomposition method at times when a particular contribution is negligibly small. Note that as the EOF decomposition technique uses a subset of the total data that is a constant depth from the surface down, this leaves a small number of points near the seabed unseparated by this analysis; these are dealt with by assuming that the wave contribution is zero at these points and setting $k_t = k_{ADCP}$.

## IV. Summary and Discussion

We have examined a set of estimated TKE values from an ADCP deployed off the Welsh coast for a period covering roughly four spring-neap cycles, which is sufficiently long to capture all the most important modes of tidal variability. The method for estimating TKE from the ADCP measurements was the standard variance method (2) [8,9], but as we discussed in section II-B this estimate is prone to contamination from wave action. Since the site at which the ADCP was deployed was reasonably exposed to waves, and we had independent measurements of wave activity from a simultaneously-deployed buoy, this dataset offered a very good opportunity to investigate how well we can determine the true TKE from the estimate that the variance method actually yields.

It is evident that the estimated TKE $k_{ADCP}$ is clearly strongly influenced by waves (fig. 2) and that since these waves are consistent with what is expected of swell waves for the location in question (fig. 3) we can surmise that this kind of wave influence is not atypical of other non-sheltered energetic tidal sites. We were also able to show, by considering a single point in time (fig. 4) that the

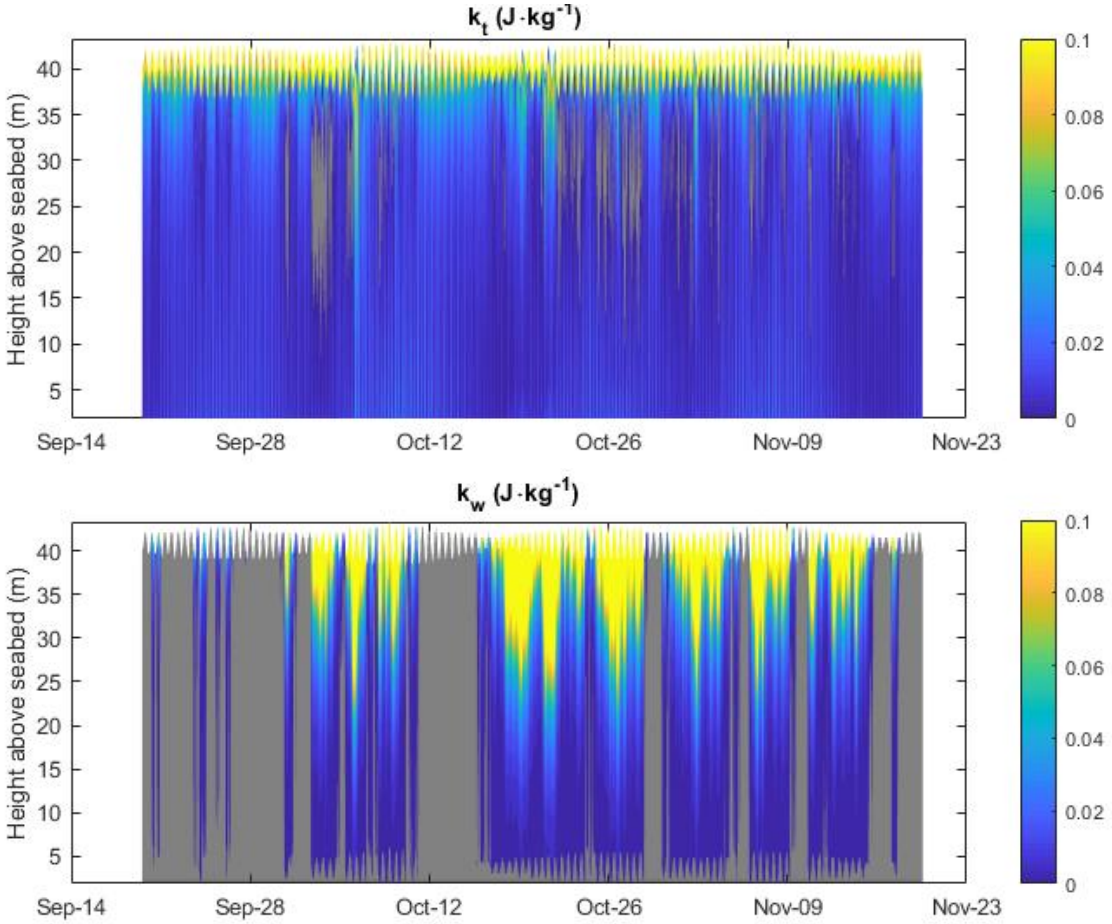


Fig. 11: Separation of the ADCP-measured pseudo-TKE (cf. fig. 2, bottom panel) into turbulent ($k_t$) and wave ($k_w$) contributions. Values below zero in either component are shown in grey.

vertical profile of $k_{ADCP}$ is consistent with the presumption of significant wave activity, not only in general shape but also in approximate magnitude when compared to linear theory.

A significant shortcoming of the EOF method for this purpose is that it is only able to capture modes within the dataset that correspond to anomalies from its time-average value. This means that, although it is theoretically capable of separating out the variation in $k_{ADCP}$ that is due to waves rather than turbulence, it cannot do anything about the bias that wave action introduces to the time-average. We have attempted to work around this obstacle by calculating a mean $k_{ADCP}$ profile based only on data from times of low wave action, and assuming that with an appropriate re-weighting based on tidal phase, this mean profile is a good approximation to that portion of mean $k_{ADCP}$ attributable to turbulence alone. The results in fig. 5 show that this approach seems to be partially successful: the portion of the mean profile that we presume to be attributable to turbulence exhibits little obviously wave-like behaviour except very near the surface. However, there are also some missing features that we would expect to see such as an increase in TKE near the bed (although this may be missing simply because since the data does not extend all the way to the bed) and, most importantly, we have no independent means of verifying the validity of this decomposition of the mean profile.

It is difficult to consider the effectiveness of the EOF analysis at separating waves and turbulence across the whole duration of the record; as a high-level overview we considered what the EOF analysis predicts to be the value of the near-surface pseudo-TKE due to wave action. In fig. 6 this was compared to the significant wave height as measured from the buoy, as well as the corresponding near-surface wave pseudo-TKE obtained from applying Airy wave theory to the buoy measurements. This showed that the statistical and theoretical predictions of wave pseudo-TKE tracked one another very closely.

A more detailed examination of the error, as illustrated by the results shown in figs. 7-10, revealed a more complex picture. Although the absolute error is never very high, the relative error between the EOF estimate of wave pseudo-TKE and the linear theory estimate can spike very high – this motivated us to discuss possible criteria for times when it may not be suitable to use these methods to estimate wave pseudo-TKE. We suggest that estimates at times when $\mathrm{EC}_1 < 0$ i.e., when the first EOF mode is negative, may not be particularly meaningful. Excluding these times results in a sharp decline in the mean error between the two estimation methods.

This examination of the error indicates that we may be able to pick out the wave contribution to the ADCP estimate of TKE. In fig. 11 we present a decomposition of the $k_{ADCP}$ data set into turbulent and wave components, based on the EOF analysis method. Note that this method uses only data from the ADCP; the wave buoy data is used only to measure the wavenumber, significant wave height and frequency that go into the linear theory estimate of the wave pseudo-TKE. This means that we could still carry out this decomposition on another measurement campaign even if there were no independent measurements of wave properties.

The decomposition appears to be quite successful: looking at the turbulent component in the top panel of fig. 11 shows very little obvious traces of wave activity except very near the surface, and a few anomalous transient features (e.g., around Oct. 5th) that may be wave-related. This may be due to the first EOF mode not capturing the whole of the wave physics: there may be higher modes that correct these transient spikes but are otherwise negligible. A detailed investigation of this is a topic for future work.

One feature of the decomposition that merits further refinement is the fact that the individual wave or turbulent contributions drop below zero at several points (the grey areas in fig. 11). This occurs because the decomposition is statistical, rather than physical; when the physical $k_t$ or $k_w$ becomes very small, the uncertainty in the decomposition method means that the statistical estimate of $k_t$ or $k_w$ may be negative. The sum of the two contributions always sums identically to the original $k_{ADCP}$ estimate, and this never drops below zero; nonetheless, it would be preferable if the two components of the decomposition were to retain this property.

## V. CONCLUSIONS

In general, both waves and turbulence act at energetic tidal sites, and both are significant environmental factors affecting TEC fatigue and reliability. The relative importance of waves and turbulence for a given TEC will be different depending on its design – most importantly, whether it is affixed to the bed or mounted on a floating hull. We therefore wish to be able to separately measure the effects of waves and turbulence at an energetic site.

It is possible to measure wave properties alone using a wave buoy, although the strong currents associated with tidal energy sites frequently cause practical problems for buoys e.g., being dragged down at the limits of their mooring. These problems may be possible to overcome with acoustic instruments incorporating a vertical beam, as previous study has shown that the vertical beam does not greatly improve estimates of turbulent properties [13].

Turbulence alone, however, cannot be measured with the bed-mounted ADCPs that are typical of site measurements (and indeed recommended by the relevant IEC standards [4]). The measurements from these devices rely on velocity variance, and thus will not yield an estimate of the true turbulent kinetic energy, but rather a quantity that includes contributions from both turbulence and waves. The study presented in this paper indicates that, where the wave contribution to this estimate significantly swamps the turbulent contribution for at least some times, empirical orthogonal function analysis will find a data mode that appears to contain most of the wave contribution and therefore permits a statistical (if not

strictly physical) separation of the wave and turbulent effects. This method can be applied even if there is no independent measurement of the wave properties from a buoy.

There are other possible techniques for decoupling waves and turbulence. As there are canonical spectra for both of these phenomena, it may be possible to carry out some form of parameter fitting to the measured combined spectra to separate waves and turbulence, if we assume there is limited non-linear interaction. We could also attempt a time-domain subtraction, although this would be highly sensitive to phase errors. An interesting potential approach to fully understanding the sensitivity of all these different techniques to errors would be virtual ADCP sampling of constructed velocity fields [19].

Nonetheless, the current study demonstrates that conventional signal separation techniques have some capacity to decouple waves and turbulence at energetic tidal sites. Further investigation can only improve our ability to decouple these phenomena.

## REFERENCES


[1] I. Milne, A. Day, R. Sharma and R. Flay, "The characterisation of the hydrodynamic loads on tidal turbines due to turbulence," *Renew. Sust. Energ. Rev.*, vol. 56, pp. 851-864, 2016

[2] F. Elasha, D. Mba, M. Togneri, I. Masters and J. Teixeira, "A hybrid prognostic methodology for tidal turbine gearboxes," *Renew. Energ.*, vol. 114, pp. 1051-1061, 2017

[3] G. N. McCann, "Tidal current turbine fatigue loading sensitivity to waves and turbulence – a parametric study," in *Proceedings of the 7th European Wave and Tidal Energy Conference*, 2007.

[4] *Tidal Energy Resource Assessment and Characterisation*, IEC/TS 62600-201:2014

[5] A. Bouferrouk, J.-B. Saulnier, G. H. Smith and L. Johanning, "Field measurements of surface waves using a 5-beam ADCP," *Ocean Eng.*, vol. 112, pp. 173-184, 2016

[6] J. M. McMillan and A. E. Hay, "Spectral and Structure Function Estimates of Turbulence Dissipation Rates in a High-Flow Tidal Channel Using Broadband ADCPs,"*J. Atmos. Ocean Tech.*, vol. 34, no. 1, pp. 5-20, 2017

[7] M. Guerra and J. Thomson, "Turbulence Measurements from Five-Beam Acoustic Doppler Current Profilers," *J. Atmos. Ocean Tech.*, vol. 34, no. 6, pp. 1267-1284, 2017

[8] M. T. Stacey, S. G. Monismith and J. R. Burau, "Measurements of Reynolds stress profiles in unstratified tidal flow," *J. Geophys. Res.*, vol. 104, pp. 10933-10949, 1999

[9] Y. Lu and R. Lueck, "Using a broadband ADCP in a tidal channel. Part II: Turbulence," *J. Atmos. Ocean Tech.*, vol. 16, no. 11, pp. 1568-1579, 1999

[10] M. Togneri, M. Lewis, S. Neill and I. Masters, "Comparison of ADCP observations and 3D model simulations of turbulence at a tidal energy site," *Renew. Energ.*, vol. 114, pp. 273-282, 2017

[11] M. Lewis, S. P. Neill, P. E. Robins and S. L. Ward, "Observations of Flow Characteristics at Potential Tidal-Stream Energy Sites," *Proceedings of the 11th European Wave and Tidal Energy Conferece*, 2015

[12] M. Piano, S. Ward, P. Robins, S. Neill, M. Lewis, A. Davies, B. Powell, A. W. Owen and R. Hashemi, "Characterizing the tidal energy resource of the West Anglesey Demonstration Zone (UK) using TELEMAC-2D and field observations," *Proceedings of the XXII TELEMAC-MASCARET Technical User Conference*, 2015

[13] M. Togneri, D. Jones, S. Neill, M. Lewis, S. Ward, M. Piano and I. Masters, "Comparison of 4- and 5-beam acoustic Doppler current profiler configurations for measurement of turbulent kinetic energy," *Enrgy. Proced.*, vol 125, pp. 260-267, 2017

[14] H. Björnsson and S. A. Venegas, "A Manual for EOF and SVD Analyses of Climatic Data," McGill University, February 1997. [Online]. Available: http://www.geog.mcgill.ca/gec3/wp-content/uploads/2009/03/Report-no.-1997-1.pdf

[15] R. W. Preisendorfer, *Principal Component Analyses in Meteorology and Oceanography*. Elsevier, 1988.

[16] I. T. Jolliffe, *Principal Component Analysis*. Springer-Verlag, 1986.

[17] G. F. Appell, P. D. Bass and M. A. Metcalfe, "Acoustic Doppler Current Profiler Performance in Near Surface and Bottom Boundaries," *IEEE J. Ocean. Eng.*, vol. 26, no. 4, pp. 390-396, 1991

[18] E. A. Nystrom, C. R. Rehmann and K. A. Oberg, "Evaluation of Mean Velocity and Turbulence Measurements with ADCPs," *J. Hydraul. Eng.*, vol. 133, no. 12, pp. 1310-1318, 2007

[19] G. Crossley, A. Alexandre, S. Parkinson, A. H. Day, H. C. M. Smith and D. M. Ingram, "Quantifying uncertainty in acoustic measurements of tidal flows using a 'Virtual' Doppler Current Profiler," *Ocean Eng.*, vol. 137, no. 1, pp. 404-416, 2017